



## Measurement of Branching Ratio $\text{Br}(B_s^0 \rightarrow D_s^{(*)} D_s^{(*)})$ with the DØ Experiment

The DØ Collaboration

URL: <http://www-d0.fnal.gov>

(Dated: March 21, 2006)

The branching ratio  $\text{Br}(B_s^0 \rightarrow D_s^{(*)} D_s^{(*)})$  was measured in a data sample collected by the DØ experiment in 2002-2005 corresponding to an integrated luminosity of approximately  $1 \text{ fb}^{-1}$ . The channel  $D_s^{(*)} D_s^{(*)}$  was selected in the state  $\mu\nu\phi D_s^{(*)}$ . The branching ratio was measured to be  $\text{Br}(B_s^0 \rightarrow D_s^{(*)} D_s^{(*)}) = 0.071 \pm 0.032(\text{stat})_{-0.025}^{+0.029}(\text{syst})$ . Since the  $D_s^{(*)} D_s^{(*)}$  system produced by the  $B_s^0$  decay is mainly in the CP-even final state, this measurement provides an estimate of the width difference  $\Delta\Gamma_{CP}$  in the  $B_s^0 - \bar{B}_s^0$  system. We find  $\Delta\Gamma_{CP}/\Gamma(B_s^0) = 0.142 \pm 0.064(\text{stat})_{-0.050}^{+0.058}(\text{syst})$ .

*Preliminary Results for Winter 2006 Conferences*

## I. INTRODUCTION

The mixing effects in  $B_s^0 - \bar{B}_s^0$  system can produce a large width difference  $\Delta\Gamma_s$  between the mass eigenstates. The simultaneous measurement of  $\Delta\Gamma_s$  and the mass difference  $\Delta m_s$  provides an important test of the Standard Model. Along with the direct measurement e.g. in the decay  $B_s^0 \rightarrow J/\psi\phi$  [1, 2],  $\Delta\Gamma_s$  can be estimated from the branching ratio  $\text{Br}(B_s^0 \rightarrow D_s^{(*)}D_s^{(*)})$  [3, 4]. This decay is predominantly CP even [3] and gives the largest contribution in the lifetime difference between  $B_s^0(\text{short})$  and  $B_s^0(\text{long})$ . The following relation can be obtained [4]:

$$2\text{Br}(B_s^0 \rightarrow D_s^{(*)}D_s^{(*)}) \simeq \frac{\Delta\Gamma_{CP}}{\Gamma} \left[ 1 + \mathcal{O}\left(\frac{\Delta\Gamma}{\Gamma}\right) \right], \quad (1)$$

where  $\Delta\Gamma_{CP} = \Delta\Gamma/\cos\phi$ . The phase  $\phi$  is related to CP violation in  $B_s^0$  mixing and is expected to be small in the SM. Only one measurement of  $\text{Br}(B_s^0 \rightarrow D_s^{(*)}D_s^{(*)})$  has been previously published [6] which was obtained from the study of correlated production of  $\phi\phi$  in  $Z^0$  decays.

This paper presents the measurement of  $\text{Br}(B_s^0 \rightarrow D_s^{(*)}D_s^{(*)})$  performed using a data sample collected by the DØ experiment in 2002-2005 corresponding to an integrated luminosity of approximately  $1\text{fb}^{-1}$ . In this decay the symbol  $D_s^{(*)}$  denotes either  $D_s$  or  $D_s^*$ . We reconstruct one  $D_s$  decaying to  $\phi\pi$  and another  $D_s$  decaying to  $\mu\phi\nu$ . Both  $\phi$  mesons decay to  $K^+K^-$ .

Events containing a muon and  $D_s \rightarrow \phi\pi$  candidates were selected and are referred to as the  $(\mu D_s)$  sample throughout. They are produced mainly by the  $B_s^0 \rightarrow \mu\nu D_s^{(*)}$  decay, with a small contribution of  $c\bar{c} \rightarrow \mu\nu D_s^{(*)}$  and of double charm decays  $B \rightarrow D_s^{(*)}D_x Y$ , with  $D_x$  decaying inclusively to a muon. A search for an additional  $\phi$  meson associated with the  $(\mu D_s)$  system was performed, and we refer to this subset sample as the  $(\mu\phi D_s)$  sample. It contains both  $B_s^0 \rightarrow D_s^{(*)}D_s^{(*)}$  decays and the contribution of different background processes. Both  $(\mu D_s)$  and  $(\mu\phi D_s)$  samples contain a large contribution of combinatoric background. The number of  $(\mu D_s)$  and  $(\mu\phi D_s)$  signal events were estimated using the fitting procedure described in Section III. The number of  $B_s^0 \rightarrow \mu D_s^{(*)}\nu$  decays in the  $(\mu D_s)$  sample and the number of  $B_s^0 \rightarrow D_s^{(*)}D_s^{(*)}$  events in the  $(\mu\phi D_s)$  sample were determined by subtracting the contribution of all other possible sources from each sample. Using the numbers of events obtained from the above procedure, the following ratio can be determined:

$$R = \frac{\text{Br}(B_s^0 \rightarrow D_s^{(*)}D_s^{(*)}) \cdot \text{Br}(D_s \rightarrow \phi\mu\nu)}{\text{Br}(B_s^0 \rightarrow \mu\nu D_s^{(*)})}. \quad (2)$$

In this ratio many detector related systematic uncertainties cancel. Using the measured value of  $R$ , PDG [5] values for  $\text{Br}(D_s \rightarrow \phi\mu\nu)$ ,  $\text{Br}(B_s^0 \rightarrow \mu\nu D_s^{(*)})$  and the new BaBar measurement [7] of  $\text{Br}(D_s \rightarrow \phi\pi)$  were used to compute  $\text{Br}(B_s^0 \rightarrow D_s^{(*)}D_s^{(*)})$ .

The selection of  $(\mu D_s)$  and  $(\mu\phi D_s)$  candidates is discussed in Section II. The procedure to obtain the number of  $(\mu D_s)$  and  $(\mu\phi D_s)$  signal events is described in Section III, and the composition of the samples is discussed in Section IV. The obtained result is given in Section V, and the systematic uncertainties are discussed in Section VI.

## II. EVENT SELECTION

The DØ detector is described in detail elsewhere [8]. A summary of the selection criteria used in the analysis are displayed in Table I. The selection criteria for the  $(\mu D_s)$  sample follow those used in a separate analysis [9] where the same decay mode  $B_s^0 \rightarrow \mu\nu D_s$ ,  $D_s \rightarrow \phi\pi$ ,  $\phi \rightarrow K^+K^-$  was used. In each event at least one muon identified by the standard DØ algorithm with  $p_T > 2\text{GeV}/c$ ,  $p > 3\text{GeV}/c$  and with at least two hits in the muon chambers was required. Two oppositely charged particles with  $p_T > 0.8\text{GeV}/c^2$  were selected among all remaining particles in the event and were each assigned the mass of a kaon. An invariant mass of  $1.01 < M(K^+K^-) < 1.03\text{GeV}/c^2$  was required for the  $K^+K^-$  system, to be consistent with the mass of a  $\phi$  meson. For each kaon candidate, the axial  $\delta_T$  [13] and stereo  $\delta_L$  [14] projections of its track impact parameter with respect to the primary vertex, together with the corresponding errors ( $\sigma(\delta_T)$ ,  $\sigma(\delta_L)$ ) were determined. The significance with respect to the primary vertex ( $S_K$ ) was defined as:

$$S_K = (\delta_T/\sigma(\delta_T))^2 + (\delta_L/\sigma(\delta_L))^2. \quad (3)$$

Both kaons were required to have  $S_K > 4$ . Each pair of kaons satisfying these criteria were combined with a third particle with  $p_T > 1.0\text{GeV}/c^2$ , which was assigned the mass of pion. The muon and pion were required to have

TABLE I: Summary of the selection criteria used in the final analysis. Nomenclature is defined in Section II.

Particle	Selection Cut
All tracks:	Number of axial hits in SMT $\geq 2$ Number of axial hits in CFT $\geq 2$
Muon:	$p_T > 2$ GeV/c $p > 3$ GeV/c Number of muon chamber hits $\geq 2$
Pion:	$p_T > 1.0$ GeV/c Opposite charge combination ( $\mu^\pm, \pi^\mp$ )
$K^\pm$ :	$p_T > 0.8$ GeV/c
$\phi$ :	Both kaons to have $S_K > 4$ , as defined in Eq. 3 Opposite kaon charge combination
$\phi$ from $D_s \rightarrow \phi\pi$ :	$1.01 < m(KK) < 1.03$ GeV/c <sup>2</sup>
$\phi$ from $D_s \rightarrow \phi\mu$ :	$0.998 < m(KK) < 1.07$ GeV/c <sup>2</sup>
$D_s \rightarrow \phi\pi$ :	$1.7 < m(\phi\pi) < 2.3$ GeV/c $\chi^2(\text{vertex}) < 16$ $d_T^D/\sigma(d_T^D) > 4$ $\cos(\alpha_T^D) > 0.9$ Helicity between $D_s$ and $K$ , $ \cos(\theta)  > 0.35$
$D_s \rightarrow \phi\mu\mu$	$1.2 < m(\phi\mu) < 1.85$ GeV/c <sup>2</sup> $\chi^2(\text{vertex}) < 16$ $d_T^D/\sigma(d_T^D) > 1$
$B_s^0 \rightarrow \mu D_s$ :	$\chi^2(\text{B vertex}) < 16$ $m(\mu D_s) < 5.2$ GeV/c <sup>2</sup> $d_T^B < d_T^D$ or $d_T^{BD} < 2 \cdot \sigma(d_T^{BD})$ $L(\mu D_s) = M(B_s) \cdot d_T^B/P_T(\mu D_s) > 150\mu\text{m}$
$B_s^0 \rightarrow \mu\phi D_s$ :	$\chi^2(\text{B vertex}) < 16$ $4.3 < m(\mu\phi D_s) < 5.2$ GeV/c <sup>2</sup> $d_T^B < d_T^D$ or $d_T^{BD} < 2 \cdot \sigma(d_T^{BD})$ $L(\mu\phi D_s) = M(B_s) \cdot d_T^B/P_T(\mu\phi D_s) > 150\mu\text{m}$

opposite charge. Each of the four particles should have at least two axial hits in the silicon microstrip tracker (SMT) and two axial hits in the central fiber tracker (CFT). The two kaons and pion were required to come from the same  $D_s(\phi\pi)$  vertex, with the  $\chi^2$  of the vertex fit  $\chi^2 < 16$ . The distance  $d_T^D$  in the axial plane between the  $D_s$  vertex and the primary interaction point was required to be  $d_T^D/\sigma(d_T^D) > 4$ . The angle  $\alpha_T^D$  between the momentum direction of a  $D_s$  candidate and the direction from the primary to the  $D_s(\phi\pi)$  vertex in the axial plane was required to be  $\cos(\alpha_T^D) > 0.9$ . A  $D_s$  candidate was constructed by combining the two kaons and the pion.

A helicity angle  $\theta$ , defined as the angle between the momenta of the  $D_s$  and a  $K$  meson in the  $(K^+, K^-)$  center of mass system was required to satisfy the condition  $|\cos(\theta)| > 0.35$ . This selection cut is motivated by the decay of  $D_s \rightarrow \phi\pi$ , which has a helicity distribution following  $\cos^2(\theta)$  compared to a uniform background distribution. The obtained sample of events satisfying these criteria were used to construct both the  $(\mu D_s)$  and  $(\mu\phi D_s)$  candidates.

To construct a  $(\mu D_s)$  candidate, the  $D_s(\phi\pi)$  candidate was required to have a common  $B$  vertex with the muon and a  $\chi^2$  of the vertex fit  $\chi^2 < 16$ . The distance  $d_T^B$  between the primary and the  $B$  vertex in the axial plane was allowed to be greater than  $d_T^D$ , provided that the distance between B and D vertices  $d_T^{BD}$  was less than  $2 \cdot \sigma(d_T^{BD})$ . The visible proper decay length defined as:

$$L(\mu D_s) = M(B_s) \cdot d_T^B/P_T(\mu D_s)$$

was required to exceed  $150\mu\text{m}$  to suppress “ $c\bar{c}$ ” contamination, as discussed in Section IV. The mass of the  $(\mu D_s)$  system was required to be less than  $5.2$  GeV/c<sup>2</sup>. Events satisfying all these criteria are referred to as the  $(\mu D_s)$  sample. The resulting mass spectrum of the  $(K^+K^-\pi)$  system with  $1.01 < M(K^+K^-) < 1.03$  GeV/c<sup>2</sup> is shown in Fig. 1. The signals of  $D_s \rightarrow \phi\pi$  and  $D^\pm \rightarrow \phi\pi^\pm$  are clearly seen. Fig. 2 shows the  $(K^+K^-)$  mass distribution for all events with  $1.92 < M(K^+K^-) < 2.0$  GeV/c<sup>2</sup>. The signal of  $\phi \rightarrow K^+K^-$  is clearly identified.

To construct a  $(\mu\phi D_s)$  candidate, an additional  $\phi$  meson was required. The selection criteria to reconstruct the second  $\phi$  are identical to that of the first  $\phi$  meson with the exception that a wider mass range  $0.998 < M(K^+K^-) < 1.07$  GeV/c<sup>2</sup> was used. This wide window was necessary to estimate the background under the  $\phi$  meson using the fitting procedure described in Section III. These two kaons and the muon were required to have a common  $D_s(\mu\phi)$

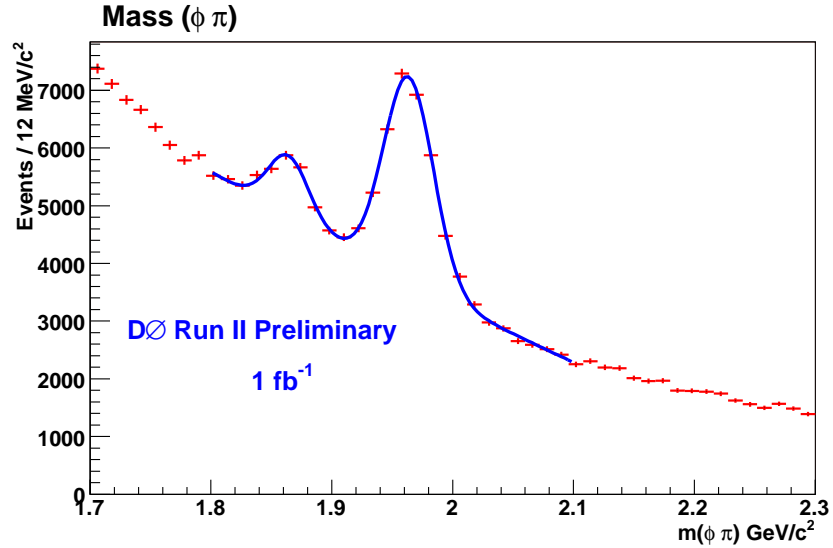


FIG. 1: Mass spectrum of  $(K^+K^-\pi)$ . Fitted function is of two Gaussians for  $D_s$  and  $D$  signals, and a 2nd-order polynomial for background. There are a total of 200k events in the histogram.

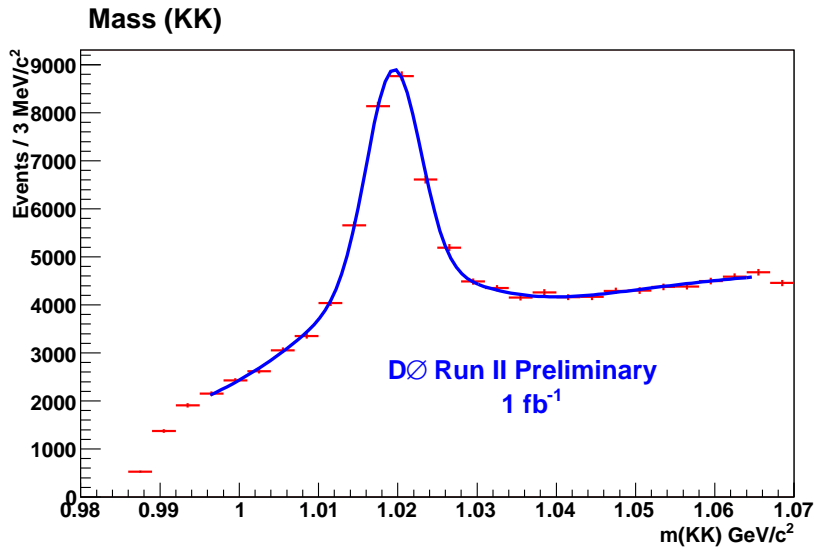


FIG. 2: Mass spectrum of  $(K^+K^-)$ . Fitted function is a double Gaussian for signal and a 2nd-order polynomial as background.

vertex with the  $\chi^2$  of the vertex fit  $\chi^2 < 16$ . The distance  $d_T^D$  in the axial plane between the  $D_s(\mu\phi)$  vertex and the primary interaction point was required to be  $d_T^D/\sigma(d_T^D) > 1$ . The mass of  $(\mu\phi)$  system for  $D_s \rightarrow \mu\phi\nu$  decay is not able to exceed the mass of the  $D_s$  meson, while background processes may have a higher  $(\mu\phi)$  mass. To suppress the background the mass of the  $(\mu\phi)$  system was required to be  $1.2 < M(\mu\phi) < 1.85 \text{ GeV}/c^2$ .

The  $D_s(\phi\pi)$  and  $D_s(\phi\mu)$  candidate were required to have a common  $B$  vertex with the  $\chi^2$  of the vertex fit  $\chi^2 < 16$ . The distance  $d_T^B$  between the primary and  $B$  vertex in the axial plane was allowed to be greater than the distance  $d_T^D$  to any of two  $D_s$  candidates provided that the distance between  $B$  and  $D$  vertices  $d_T^{BD}$  was less than  $2 \cdot \sigma(d_T^{BD})$ . The visible proper decay length defined as:

$$L(\mu\phi D_s) = M(B_s) \cdot d_T^B / P_T(\mu\phi D_s)$$

was required to exceed  $150 \mu\text{m}$ . This cut was the same as for the  $(\mu D_s)$  system and was applied to suppress both the “ $c\bar{c}$ ” background and  $\phi$  mesons from fragmentation, as each originate from the primary interaction and produce

a small pseudo proper decay length.

The simulation of the  $B_s^0 \rightarrow D_s^{(*)} D_s^{(*)}$  decay shows that the mass of the  $(\mu\phi D_s)$  system after all these selections tends to have high values. Therefore the mass of the  $(\mu\phi D_s)$  system was required to be  $4.3 < M(\mu\phi D_s) < 5.2$  GeV. Events satisfying all these criteria are referred to as the  $(\mu\phi D_s)$  sample.

### III. FITTING PROCEDURE

The selected  $(\mu D_s)$  and  $(\mu\phi D_s)$  samples contain both signal and background events. The fitting procedure described in this Section was applied to extract the number of  $(\mu D_s)$  and  $(\mu\phi D_s)$  signal events.

The number of  $(\mu D_s)$  events is estimated from a binned fit to the  $(K^+ K^- \pi^\pm)$  mass distribution shown in Fig. 1. Two Gaussians were used to describe the  $D^\pm \rightarrow \phi \pi^\pm$  and  $D_s^\pm \rightarrow \phi \pi^\pm$  decays, and a 2nd-order polynomial was used to parameterize the background. The result of this fit is superimposed in Fig. 1 as a solid line. The fit gives:

$$N(\mu D_s) = 15225 \pm 310. \quad (4)$$

To extract the number of  $(\mu\phi D_s)$  events an unbinned Log-Likelihood fit was used. The two variables fitted were the mass  $M_D$  of the  $(\phi\pi)$  system and the mass  $M_\phi$  of the two additional kaons from the  $(\phi\mu)$  system. All events from the  $(\mu\phi D_s)$  sample with  $1.7 < M_D < 2.3$  GeV/c<sup>2</sup> and  $0.998 < M_\phi < 1.07$  GeV/c<sup>2</sup> were included in the fit. The probability density function  $\mathcal{F}_S$  to observe the masses  $M_D$  and  $M_\phi$  is given by:

$$\begin{aligned} \mathcal{F}_S(M_D, M_\phi) &= G_D(M_D, \hat{M}_D, \sigma_D) G_\phi(M_\phi, \hat{M}_\phi, \sigma_1, \sigma_2, h), \\ G_D(M, \hat{M}, \sigma) &= \frac{1}{\sqrt{2\pi}\sigma} \exp\left(-\frac{(M - \hat{M})^2}{2\sigma^2}\right), \\ G_\phi(M, \hat{M}, \sigma_1, \sigma_2, h) &= \frac{h}{\sqrt{2\pi}\sigma_1} \exp\left(-\frac{(M - \hat{M})^2}{2\sigma_1^2}\right) + \frac{(1-h)}{\sqrt{2\pi}\sigma_2} \exp\left(-\frac{(M - \hat{M})^2}{2\sigma_2^2}\right). \end{aligned} \quad (5)$$

Here a single Gaussian is used to describe the  $D_S$  signal and a double Gaussian for the  $\phi$  peak. In  $G_\phi$ ,  $\sigma_1$  and  $\sigma_2$  are the narrow and wide widths, and  $h$  is defined as the fraction of signal from the narrow Gaussian.

The probability density function for combinatorial background in each variable was parametrized by:

$$\begin{aligned} \mathcal{F}_B(M, a, b) &= \frac{1}{n} (1 + a M + b M^2), \\ n &= \int_{M_{low}}^{M_{high}} dM (1 + a M + b M^2). \end{aligned} \quad (6)$$

The resulting PDF describing the distribution of  $(M_D, M_\phi)$  is given by:

$$\begin{aligned} \mathcal{F}(M_D, M_\phi) &= f_s \mathcal{F}_s(M_D, M_\phi) + \\ &f_\phi \mathcal{F}_B(M_D, a_D, b_D) G_\phi(M_\phi, \hat{M}_\phi, \sigma_1, \sigma_2, h) + \\ &f_D \mathcal{F}_B(M_\phi, a_\phi, b_\phi) G_D(M_D, \hat{M}_D, \sigma_D) + \\ &(1 - f_s - f_\phi - f_D) \mathcal{F}_B(M_D, a_D, b_D) \mathcal{F}_B(M_\phi, a_\phi, b_\phi). \end{aligned} \quad (7)$$

In this expression the second term describes the production of a  $\phi$  meson without a  $D_s(\phi\pi)$ , and the third term describes the production of  $D_s(\phi\pi)$  without an additional  $\phi$  meson. The parameters  $f_s, f_\phi$ , and  $f_D$  refer to the fraction of events from signal,  $\phi$  and  $D_s$  production and are extracted from the fit. The Likelihood function used in the fit is given by:

$$\mathcal{L} = \prod_{i=1}^N \mathcal{F}^i(M_D, M_\phi), \quad (8)$$

where the product was taken over all selected events  $N$ .

In the fitting procedure,  $\hat{M}$  and  $\sigma$  for both  $D_s$  and  $\phi$  signals were fixed to the parameters extracted from a fit to the  $(\mu D_s)$  data sample shown in Figs. 1–2. In the  $\phi$  signal the relative fraction  $h$  was also fixed. The background polynomial coefficients and  $f_i$  were allowed to float. The  $D^\pm$  peak is not included in the fit as no structure is visible

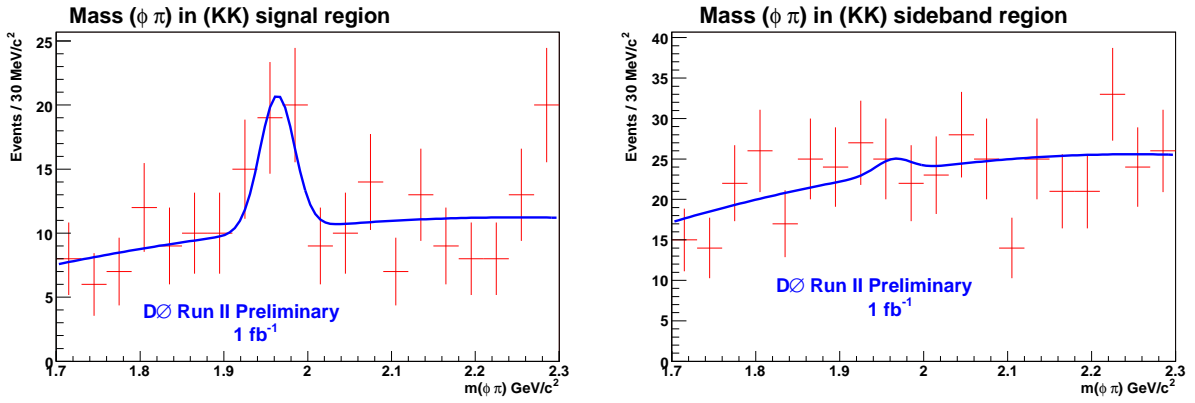


FIG. 3: Mass plot of  $(\phi\pi)$ . The left plot contains events from the  $(KK)$  signal region. The right plot is constructed from events in the  $(KK)$  sideband mass window. The curves displayed in the plots correspond to the fitted result of the unbinned Log-Likelihood fit.

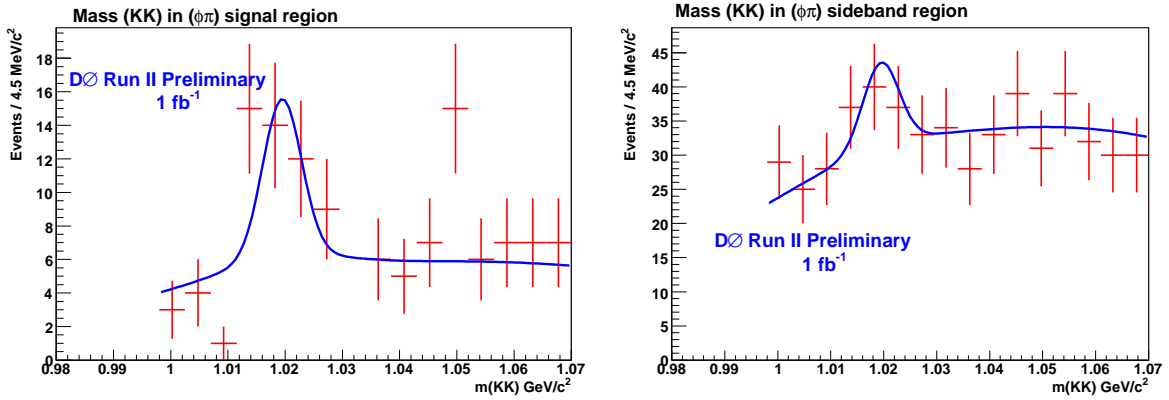


FIG. 4: Mass plot of  $(KK)$  for  $D_s^{(*)} \rightarrow \phi\mu$ . The left histogram contains events from the  $(\phi\pi)$  signal region and events from the  $(\phi\pi)$  sideband region are displayed in the right plot. The superimposed curves are projections from the unbinned Log-Likelihood fit.

(see Fig. 3). In the fitting procedure the values of  $f_i$  were constrained to remain in the range from zero to one. The number of  $(\mu\phi D_s)$  events was determined from:

$$N(\mu\phi D_s) = f_s N. \quad (9)$$

Fig. 3 shows the distribution of the  $(\phi\pi)$  mass when the mass of the second pair of kaons is  $1.01 < M(K^+K^-) < 1.03$   $\text{GeV}/c^2$  (left plot) or outside this range (right plot). Fig. 4 shows the distribution of the mass of the second pair of kaons when  $1.92 < M(\phi\pi) < 2.0$   $\text{GeV}/c^2$  (left plot) or outside this range (right plot). The superimposed curves are projections of the fit onto the mass spectrum having integrated out the other mass variable over its signal or sideband region. The correlated production of  $\phi$  and  $D_s$  is clearly seen. The fit gives:

$$N(\mu\phi D_s) = 19.34 \pm 7.85. \quad (10)$$

The significance of this fit is 2.77 and was determined by comparison to the fit when the signal fraction  $f_s$  is fixed to zero.

As a consistency check, a similar sample was obtained using the same criteria for the selection of  $(\mu\phi D_s)$  candidates with the exception that in this case the muon and  $D_s$  candidate were required to have the same charge. When applying the same Log-Likelihood fit as before, the number of  $\mu^+\phi D_s^+$  was found to be at the lower limit with an error of 19 events. It should also be noted that no contribution of  $D^+ \rightarrow \phi\pi^+$  in the  $(\mu\phi D_s)$  sample was observed (see Fig. 3).

TABLE II: The reconstruction rate of different processes relative to  $B_s^0 \rightarrow \mu\nu D_s^{(*)}$ . The production and branching ratios used [5, 10] are also given.

Process	$f(b \rightarrow B)$	Branching ratio (%)	$r_i$
$B^0 \rightarrow D_s D^{(*)} X$	0.397	$10.5 \pm 2.6$	$0.082 \pm 0.020$
$B^\pm \rightarrow D_s D^{(*)} X$	0.397	$10.5 \pm 2.6$	$0.082 \pm 0.020$
$B_s^0 \rightarrow D_s^{(*)} D_s^{(*)}$	0.107	$12_{-7}^{+11}$	$0.046 \pm 0.035$
$B_s \rightarrow D_s D X$	0.107	$15.4 \pm 15.4$	$0.023 \pm 0.023$

#### IV. SAMPLE COMPOSITION

To extract the number of  $B_s^0 \rightarrow \mu\nu D_s^{(*)}$  and  $B_s^0 \rightarrow D_s^{(*)} D_s^{(*)}$  events from Eq. 4 and 10, the composition of the selected samples needs to be determined. Since the available measurements of  $B_s^0 \rightarrow \mu\nu D_s^{(*)} X$  were semi-inclusive, the processes listed below were considered as signal and their branching rates were set in the simulation to the following values [10]:

$$\begin{aligned}
 \text{Br}(B_s^0 \rightarrow \mu\nu D_s) &= 2.10\% \\
 \text{Br}(B_s^0 \rightarrow \mu\nu D_s^*) &= 5.60\% \\
 \text{Br}(B_s^0 \rightarrow \mu\nu D_{s0}^*) &= 0.20\% \\
 \text{Br}(B_s^0 \rightarrow \mu\nu D_{s1}^*) &= 0.37\% \\
 \text{Br}(B_s^0 \rightarrow \tau\nu D_s^{(*)}) \text{ Br}(\tau \rightarrow \mu\nu) &= 0.51\%
 \end{aligned}$$

The  $D_{s0}^*$  and  $D_{s1}^*$  were each decayed to  $D_s$  and  $\pi^0$ .

The background processes and their reconstruction rates  $r_i$  relative to the defined above  $B_s^0 \rightarrow \mu\nu D_s^{(*)} X$  process are given in Table II. The  $r_i$  were defined as the ratio of efficiencies to reconstruct the corresponding processes:

$$r_i = \frac{\varepsilon(b\bar{b} \rightarrow BY \rightarrow D_s^{(*)} D_x Y')}{\varepsilon(b\bar{b} \rightarrow B_s^0 Y \rightarrow D_s^{(*)} \mu\nu Y')}$$

and were determined using the standard  $D\bar{O}$  simulation tools followed by the complete event reconstruction, and applying the same selection criteria as in data. All rates include both the production and branching ratios. The branching ratios for  $B \rightarrow D_s D^{(*)} X$  and  $B_s \rightarrow D_s D_s$  are taken from the PDG [5]. There is no experimental information for the  $\text{Br}(B_s^0 \rightarrow D_s D X)$ , therefore we used the value provided by EvtGen [10] and assigned a 100% uncertainty to this value.

In addition, the  $(\mu D_s)$  sample includes the processes  $c\bar{c} \rightarrow \mu\nu D_s X$ ,  $b\bar{b} \rightarrow \mu\nu D_s X$ , events with a misidentified muon, etc. which we refer to as “ $c\bar{c}$ ”. The distinguishing feature of  $c\bar{c}$  processes is a small pseudo-proper decay length, which is centred around zero with an RMS varying from 80 to 150  $\mu\text{m}$ , and therefore the cut  $L(\mu D_s) > 150\mu\text{m}$  was applied. With this cut, the estimated contribution of  $c\bar{c}$  processes in the  $(\mu D_s)$  sample is reduced to  $2 \pm 1\%$  for the RMS=150  $\mu\text{m}$ . In total, we estimated that the fraction of events in  $(\mu D_s)$  coming from  $B_s^0 \rightarrow \mu\nu D_s^{(*)} X$  is:

$$f(B_s^0 \rightarrow \mu\nu D_s^{(*)}) = 0.79 \pm 0.05. \quad (11)$$

For the  $(\mu\phi D_s)$  sample the contribution of the following processes were considered:

1.  $B_s^0 \rightarrow D_s^{(*)} D_s^{(*)}$  - the main process;
2.  $B \rightarrow D_s^{(*)} D_s^{(*)} K X$  - double- $D_s$  decay of ordinary  $B$  mesons;
3.  $B_s^0 \rightarrow D_s^{(*)} D_s^{(*)} X$  - multi-body double charm decays;
4.  $B_s^0 \rightarrow \mu\nu D_s^{(*)} \phi$ ;
5.  $c\bar{c} \rightarrow \mu\phi D_s^{(*)}$ ;
6.  $B_s^0 \rightarrow \mu\nu D_s^{(*)}$  and a  $\phi$  meson from fragmentation.

All these processes were simulated using the standard  $D\bar{O}$  tools and reconstructed using the same algorithms as for data. There is no experimental information for most of the processes, therefore their contribution was estimated by counting events in different regions of the  $(\mu\phi D_s)$  phase space and comparing the obtained numbers with the expected mass distribution for a given background process.

The mass of the  $(\mu\phi D_s)$  system for the second and third processes is much less than for the main decay  $B_s^0 \rightarrow D_s^{(*)} D_s^{(*)}$  because of additional non-reconstructed  $\pi\pi$  pairs or  $K$  mesons. The applied cut  $M(\mu\phi D_s) > 4.3 \text{ GeV}/c^2$  should strongly suppress them. The contribution of the  $B_s^0 \rightarrow D_s^{(*)} D_s^{(*)} X$  should be much less than  $B \rightarrow D_s^{(*)} D_s^{(*)} KX$  because of a higher production rate of  $B^+$  and  $B^0$  compared to  $B_s^0$ . The final state in the  $B_s^0 \rightarrow D_s^{(*)} D_s^{(*)} X$  decay should include at least 2  $\pi$  mesons due to isospin conservation; at least 2 gluons are required to produce this state (similar to  $\psi(2s) \rightarrow J/\psi\pi\pi$ ) and is therefore additionally suppressed. As a result, its contribution is neglected compared to the  $B \rightarrow D_s^{(*)} D_s^{(*)} KX$  process.

The simulation shows that for the  $B \rightarrow D_s^{(*)} D_s^{(*)} KX$  decay:

$$\frac{N(M(\mu\phi D_s)) > 4.3 \text{ GeV}/c^2}{N(M(\mu\phi D_s)) < 4.3 \text{ GeV}/c^2} = 0.02. \quad (12)$$

Applying the cut on  $M(\mu\phi D_s) < 4.3 \text{ GeV}/c^2$  and keeping all other selections we observe in data  $21.8 \pm 14.8$  events. The contribution of the decay  $B_s^0 \rightarrow D_s^{(*)} D_s^{(*)}$  into such a sample should be very small. Supposing that all these events come from  $B \rightarrow D_s^{(*)} D_s^{(*)} KX$  and using Eq. 12, we estimated their contribution into the signal  $(\mu\phi D_s)$  as  $0.44 \pm 0.30$  events.

The fourth process should produce the high mass of both  $(\mu\phi)$  and  $(\mu\phi D_s)$  systems. The applied cut  $M(\mu\phi) < 1.85 \text{ GeV}/c^2$  should strongly suppress it. The simulation shows that for this process:

$$\frac{N(M(\mu\phi)) < 1.85 \text{ GeV}/c^2}{N(M(\mu\phi)) > 1.85 \text{ GeV}/c^2} = 0.15. \quad (13)$$

Applying the cut  $M(\mu\phi) > 1.85 \text{ GeV}/c^2$  and keeping all other selections we observe  $8.6 \pm 7.7$  events. The contribution of the  $B_s^0 \rightarrow D_s^{(*)} D_s^{(*)}$  decay into such a sample should be very small. Assuming that all these events come from the fourth background process and using Eq. 13 we estimated its contribution to the signal  $(\mu\phi D_s)$  as  $1.27 \pm 1.14$  events.

The “ $c\bar{c}$ ” processes are strongly suppressed by the cut on the visible proper decay length. The selection of an additional  $\phi$  meson reduces the contribution of these processes to a small level. It was estimated that  $c\bar{c} \rightarrow \mu\phi D_s X$  contributes an upper limit value of  $0.36 \pm 0.36$  events, and we therefore include this error as a systematic uncertainty.

Finally, the production of a  $\phi$  meson from fragmentation is not correlated with the decay of  $B_s^0 \rightarrow \mu\nu D_s^{(*)}$  and any possible contribution of this process was taken into account by our fitting procedure. In addition, an attempt was made to reconstruct  $(\mu\phi D_s)$  events in the  $B_s^0 \rightarrow \mu\nu D_s^{(*)}$  simulation containing approximately 9200 reconstructed  $(\mu D_s)$  events, and no such events were found. Therefore the contribution of this process was neglected. In total, we estimate the number of background events in Eq. 10 as:

$$N_{bkg}(\mu\phi D_s) = 1.7 \pm 1.2. \quad (14)$$

## V. RESULTS

Using Equations 4, 10, 11 and 14 we obtained the  $\text{Br}(B_s^0 \rightarrow D_s^{(*)} D_s^{(*)})$  using:

$$\frac{N(\mu\phi D_s) - N_{bkg}(\mu\phi D_s)}{N(\mu D_s) f(B_s^0 \rightarrow \mu\nu D_s^{(*)})} = \frac{2 \text{Br}(B_s^0 \rightarrow D_s^{(*)} D_s^{(*)}) \cdot \text{Br}(D_s \rightarrow \phi\mu\nu)}{\text{Br}(B_s^0 \rightarrow \mu\nu D_s^{(*)})} \text{Br}(\phi \rightarrow K^+ K^-) \frac{\varepsilon(B_s^0 \rightarrow D_s^{(*)} D_s^{(*)})}{\varepsilon(B_s^0 \rightarrow \mu\nu D_s^{(*)})}, \quad (15)$$

where  $\varepsilon(B_s^0 \rightarrow D_s^{(*)} D_s^{(*)})/\varepsilon(B_s^0 \rightarrow \mu\nu D_s^{(*)})$  is the ratio of efficiencies to reconstruct these two processes, which was determined from simulation. Since the two selected final states differ only by an additional  $\phi$  meson, while all other applied selections are the same, many detector-related systematic uncertainties cancel in this ratio. The muon  $p_T$  spectrum in  $B_s^0 \rightarrow \mu\nu D_s^{(*)}$  decay differs in data and in simulation due to the triggers and the uncertainties in  $B$  meson production in Monte Carlo. To take into account this difference weighting functions were applied to the  $p_T$  of the  $B$  meson and also the  $p_T$  of the muon. With this correction the ratio of efficiencies was found to be:

$$\frac{\varepsilon(B_s^0 \rightarrow D_s^{(*)} D_s^{(*)})}{\varepsilon(B_s^0 \rightarrow \mu\nu D_s^{(*)})} = 0.057 \pm 0.002 \text{ (stat)}, \quad (16)$$

where the error reflects statistics from MC. A systematic uncertainty is assigned to this ratio which is discussed in Section VI.

Using all these numbers the following result was obtained:

$$R = \frac{\text{Br}(B_s^0 \rightarrow D_s^{(*)} D_s^{(*)}) \cdot \text{Br}(D_s \rightarrow \phi \mu \nu)}{\text{Br}(B_s^0 \rightarrow \mu \nu D_s^{(*)})} = 0.027 \pm 0.012 \text{ (stat)}. \quad (17)$$

The value  $\text{Br}(\phi \rightarrow K^+ K^-) = 0.491 \pm 0.007$  was taken from PDG [5]. The statistical uncertainty shown in Eq. 17 includes only the uncertainty in the number of  $(\mu \phi D_s)$  signal from Eq. 10. All other uncertainties are included in the systematics and are discussed in Section VI.

Both  $\text{Br}(B_s^0 \rightarrow \mu \nu D_s^{(*)})$  and  $\text{Br}(D_s \rightarrow \phi \mu \nu)$  depend on  $\text{Br}(D_s \rightarrow \phi \pi)$  which is given in PDG with large uncertainty:  $\text{Br}(D_s \rightarrow \phi \pi) = (3.6 \pm 0.9)\%$  [5]. This situation was significantly improved recently with the publication of the new measurement  $\text{Br}(D_s \rightarrow \phi \pi) = (4.81 \pm 0.52 \pm 0.38)\%$  by BaBar [7]. Combining it with the PDG value, we get:

$$\text{Br}(D_s \rightarrow \phi \pi) = 0.0440 \pm 0.0052. \quad (18)$$

Factorizing the dependence on  $\text{Br}(D_s \rightarrow \phi \pi)$  we obtained from the PDG results:

$$\text{Br}(B_s^0 \rightarrow \mu \nu D_s^{(*)}) \text{Br}(D_s \rightarrow \phi \pi) = (2.84 \pm 0.49) \times 10^{-3}, \quad (19)$$

$$\text{Br}(D_s \rightarrow \phi \mu \nu) = (0.55 \pm 0.04) \text{Br}(D_s \rightarrow \phi \pi). \quad (20)$$

Using these numbers, we finally obtained:

$$\text{Br}(B_s^0 \rightarrow D_s^{(*)} D_s^{(*)}) = (0.071 \pm 0.032(\text{stat})) \left( \frac{0.044}{\text{Br}(D_s \rightarrow \phi \pi)} \right)^2. \quad (21)$$

## VI. SYSTEMATIC UNCERTAINTIES

The systematic uncertainties in the measured value of  $\text{Br}(B_s^0 \rightarrow D_s^{(*)} D_s^{(*)})$  were estimated as follows. All branching ratios taken from the PDG were varied within one standard deviation. The uncertainty in  $\text{Br}(D_s \rightarrow \phi \pi)$  gives the largest contribution and is shown as a separate entry. For  $\text{Br}(D_s \rightarrow \phi \pi)$  we used the number given in Eq. 18, although our result can be easily rescaled for any other values. A 100% uncertainty in the number of background events in  $(\mu \phi D_s)$  sample was assumed. The ratio of efficiencies given in Eq. 16 can be affected by the uncertainties of reconstruction of two additional charged particles from the  $\phi$  meson decay. A different analysis [11] measured the efficiency to reconstruct a charged pion from the decay  $D^{*+} \rightarrow D^0 \pi^+$  and the obtained value was in a good agreement with the MC estimate. This comparison is valid within the uncertainty of branching ratios of different  $B$  semileptonic decays, which is about 7%. Therefore we conservatively assigned a 14% systematic uncertainty (7% for each charged particle, 100% correlated) to the ratio of efficiencies and propagated it to the final result. For the ratio of efficiencies a 15% value is assigned for the reweighting procedure, which reflects the difference in efficiency between weighted and unweighted estimates. Table III shows all obtained contributions to the systematic uncertainty.

Using these numbers, the preliminary result of this measurement is:

$$\text{Br}(B_s^0 \rightarrow D_s^{(*)} D_s^{(*)}) = (0.071 \pm 0.032(\text{stat}) \pm 0.021(\text{syst})) \left( \frac{0.044}{\text{Br}(D_s \rightarrow \phi \pi)} \right)^2. \quad (22)$$

Using the value from Eq. 18 of  $\text{Br}(D_s \rightarrow \phi \pi)$  we get:

$$\text{Br}(B_s^0 \rightarrow D_s^{(*)} D_s^{(*)}) = 0.071 \pm 0.032(\text{stat})_{-0.025}^{+0.029}(\text{syst}). \quad (23)$$

## VII. CONCLUSIONS

We measure:

$$\text{Br}(B_s^0 \rightarrow D_s^{(*)} D_s^{(*)}) = (0.071 \pm 0.032(\text{stat}) \pm 0.021(\text{syst})) \left( \frac{0.044}{\text{Br}(D_s \rightarrow \phi \pi)} \right)^2. \quad (24)$$

TABLE III: Systematic uncertainties for the  $\text{Br}(B_s^0 \rightarrow D_s^{(*)} D_s^{(*)})$ .

Source	Uncertainty in $\text{Br}(B_s^0 \rightarrow D_s^{(*)} D_s^{(*)})$
$\text{Br}(D_s \rightarrow \phi\pi) = 0.0440 \pm 0.0520$	$^{+0.020}_{-0.014}$
$\text{Br}(B_s^0 \rightarrow \mu\nu D_s^{(*)}) \text{ Br}(D_s \rightarrow \phi\pi)$	0.012
$\text{Br}(D_s \rightarrow \phi\mu\nu)/\text{Br}(D_s \rightarrow \phi\pi)$	0.005
$f(B_s^0 \rightarrow \mu\nu D_s^{(*)}) = 0.79 \pm 0.05$	0.005
Background contribution in $N(\mu\phi D_s)$	0.007
Ratio of efficiencies	0.010
Reweighting of MC	0.011

Using the  $\text{Br}(D_s \rightarrow \phi\pi)$  value given in Eq. 18, the value of  $\text{Br}(B_s^0 \rightarrow D_s^{(*)} D_s^{(*)})$  was found to be:

$$\text{Br}(B_s^0 \rightarrow D_s^{(*)} D_s^{(*)}) = 0.071 \pm 0.035(\text{stat})_{-0.025}^{+0.029}(\text{syst}). \quad (25)$$

Assuming that the relation given in Eq. 1 is correct, we get:

$$\frac{\Delta\Gamma_{CP}}{\Gamma}(B_s^0) = 0.142 \pm 0.064(\text{stat})_{-0.050}^{+0.058}(\text{syst}). \quad (26)$$

This independent estimate is in a good agreement with the SM prediction  $\Delta\Gamma/\Gamma(B_s^0) = 0.12 \pm 0.06$  [4] and with the direct measurement of this parameter by the DØ experiment in  $B_s^0 \rightarrow J/\psi\phi$  decays [2]. The agreement with the CDF measurement of  $\Delta\Gamma/\Gamma(B_s^0)$ , which was also performed in  $B_s^0 \rightarrow J/\psi\phi$  [1] is worse, although still within two standard deviations. The obtained result agrees well with the ALEPH measurement  $2 \cdot \text{Br}(B_s^0 \rightarrow D_s^{(*)} D_s^{(*)}) = 0.23 \pm 0.10_{-0.09}^{+0.19}$  [6]. This agreement is even better if the ALEPH measurement is corrected by the new value from Eq. 18 of  $\text{Br}(D_s \rightarrow \phi\pi)$ .

- 
- [1] D. Acosta *et al.* (CDF Collaboration), Phys.Rev.Lett. **94** 101803 (2005).
  - [2] V.M. Abazov *et al.* (DØ collaboration), Phys.Rev.Lett. **95** 171801 (2005).
  - [3] R. Alexan *et al.* Phys. Lett. **B316**,567 (1993).
  - [4] I. Dunietz, R. Fleischer, U. Nierste, “In pursuit of new physics with  $B_s^0$  decays”, arxiv:hep-ph/0012219.
  - [5] S. Eidelman *et al.* (Particle Data Group), Phys. Lett. **B592**, 1 (2004).
  - [6] R. Barate *et al.* (ALEPH Collaboration), Phys. Lett. **B486**, 286 (2000).
  - [7] B. Aubert *et al.* (BaBar Collaboration), Phys. Rev. D **71**, 091104 (2005).
  - [8] V.M. Abazov *et al.* (DØ collaboration), “The Upgraded DØ Detector”, arxiv: hep-physics/0507191.
  - [9] V.M Abazov *et al.* (DØ collaboration), “Mixing in the  $B_s$  System Using  $B_s$  to  $D_s\mu X$ ,  $D_s$  to  $\phi\pi$  Decay Mode And Opposite-Side Flavor Tagging”, DØ Note 4881-CONF.
  - [10] D.J.Lange, Nucl. Instrum. Meth. **A462**, 152 (2001).
  - [11] V.M. Abazov *et al.* (DØ collaboration), Phys. Rev. Lett. **94**, 182001 (2005).
  - [12] V.M. Abazov *et al.* (DØ collaboration), Phys. Rev. Lett. **94**, 232001 (2005).
  - [13] In the plane perpendicular to the beam direction.
  - [14] Parallel to the beam direction.